

1 Introduction

Soils play a major role in the global C budget, as they contain 2 to 3 times more C than the atmosphere and ca. 3 times more C than the aboveground biomass. In addition, the size of soil C pool corresponds approximately to a third of the geological reservoir present as fossil fuels (Eswaran et al., 1993; Lal et al., 2003).

Current large scale estimations of the exchange of C between the soil and the atmosphere are associated with large uncertainties (Houghton et al., 2003, 2007; Peters et al., 2010). Both modelling and experimental approaches have been applied to assess C exchange fluxes at large spatial scales. Yet these approaches are subjected to substantial limitations: (i) the current technical possibilities to measure directly hillslope aggregated CO₂ fluxes are limited (e.g. Baldocchi, 2003), and (ii) the complexity of processes at the scale of a whole catchment is not fully considered in current models of C at the soil-atmosphere interface (Chaopricha and Marín-Spiotta, 2014; Trumbore and Czimczik, 2008).

In-situ measurements of the hillslope aggregated CO₂ fluxes has been largely achieved using the Eddy-Covariance technique (e.g. Goulden et al., 1996; Eugster et al., 2010), but this technique is not appropriate for sloping landscapes, providing an uncertainty on the CO₂ fluxes ranging from 100 to 200 g C m⁻² year⁻¹ at such non-ideal sites (Baldocchi, 2003). At the local scale, more precise technologies such as survey chambers with infra-red gas analyzers (IRGA) (e.g. Davidson et al., 2002) or such as the non-dispersive infra-red (NDIR) probes (e.g. Young et al., 2009) can be used. However the support scale and spatial resolution of these devices are often too small to make robust large scale assessment of C exchanges across the soil atmosphere interface.

Alternatively, soil modeling of OC dynamics allows assessing the heterotrophic soil respiration (e.g. Herbst et al., 2008). Such models simulations have already been used to calculate the hillslope aggregated CO₂ fluxes (e.g. Dai et al., 2012). However, the predictive capabilities of the models are limited because they do not account for the

13701

varying topography and biophysical conditions across the landscape (Dai et al., 2012), and because some key mechanisms controlling the soil CO₂ efflux are not sufficiently implemented in current OC dynamic models: (i) the physical controls on CO₂ fluxes, e.g. gas diffusion barriers along soil profiles, (e.g. Ball, 2013; Maier et al., 2011; Wiaux et al., 2014c); and (ii) the contribution of buried OC at downslope depositional areas to soil C emissions (e.g. Van Oost et al., 2012; Wang et al., 2014; Wiaux et al., 2014a).

While the transfer of soil OC by erosion has been recognized (e.g. Quinton et al., 2010; Stallard, 1998), its impact on both local and global C budgets is poorly understood (Lal, 2003), and consequently not implemented in OC dynamics models. Once brought at the bottom of the slope, sediments deposits enriched in soil OC accumulate and are progressively buried deeper and deeper along the soil profiles, forming colluvic soils at the depositional site, with an increasing soil OC stock (Van Oost et al. 2005a, b, 2012; Wiaux et al., 2014a). However, a series of complex and interacting processes are acting in these depositional sites, able to decrease as well to enhance mineralization (Lal, 2003; Wiaux et al., 2014b). Recent studies (Rumpel and Kögel-Knabner, 2011) highlighted that deep soil OC is highly processed, and showed the need to study more in details the C fluxes coming from deep soil horizons. Recently, through a vertical partitioning of CO₂ fluxes along soil profiles, some authors (Takahashi et al., 2004; Davidson et al., 2006; Goffin et al., 2014) showed that the 30 first centimeters of soil significantly contribute to the total surface CO₂ flux. However, to our knowledge, such a vertical partitioning has never been carried out neither in larger scale agro-ecosystems nor in downslope colluvium with buried OC in deep soil layers.

In this study, we aim to quantify the soil-atmosphere C flux at the scale of a hillslope. More specifically, we aim to evaluate two key mechanisms able to improve this estimation of the hillslope aggregated CO₂ fluxes: (i) the persistence of OC in deep colluvium deposits through a vertical partitioning of soil CO₂ fluxes; and (ii) the physical controls on CO₂ fluxes along soil profiles.

13702

2 Material and methods

2.1 Study site description

The study was carried out in the Belgian loam belt along a cultivated hillslope of 150 m length (50.6669° N, 4.6331° W). The site has a maritime temperate climate, with an average annual temperature of 9.7 °C and an average annual precipitation of 805 mm. The study site is described in detail in Wiaux et al. (2014a, b). We selected 2 measurement stations along the hillslope: one at the summit and one at the footslope position. The soil is a Dystric Luvisol type at the summit and a Colluvic Regosol in the depositional area at the footslope (Wiaux et al., 2014a, b). The soil properties of these two soil profiles have been characterized by Wiaux et al. (2014a, b): soil total OC, labile pool OC and porosity profiles are illustrated on Figs. 1 and 2, respectively.

The total porosity (\emptyset) was measured in the laboratory by weighting 100 cm³ undisturbed soil cores both at saturation and after oven drying at 105 °C during 48 h. The \emptyset was then deduced from the mass of water needed to fill sample pores. The air-filled porosity (ε) was calculated as the difference between \emptyset and VWC. Average and standard deviation values were calculated on triplicate samples for each depth.

Soil water retention (SWR) curves were characterized using undisturbed soil cores at 10, 25, 35, 50, 70 and 95 cm depth, with 3 replicates at each depth. ε_{100} and b parameters were obtained by fitting the Campbell (1974) model of SWR curve to the SWR observations (Moldrup et al., 2000).

2.2 Monitoring of soil CO₂, water and temperature

We measured soil CO₂ concentrations by means of specific designed soil CO₂ probes. The CO₂ sensor in the probe is based on the CARBOCAP® Single-Beam Dual Wavelength non-dispersive infra-red (NDIR) technology (GMM221, Vaisala corp., Vantaa, Finland). Analytical precision is 1.5 % of the measurement range added to 2 % of the observed value. The sensor was covered with nylon and PTFE (polytetrafluoroethy-

13703

lene) membranes and encapsulated in a tube to avoid soil particles entering the sensor and to limit water infiltration. This tubing method is an adaptation of the technique presented by Young et al. (2009). These tubes were inserted vertically into the soil, after augering holes with a diameter that equals the diameter of the PVC tubes. To obtain an equilibrated soil environment around the soil concentration probe, we started measurements 1 month after the probes installation. The measurement plots were covered with a synthetic permeable geotextile during the complete measurement period (Fig. 4). This avoided vegetation growth and any autotrophic contribution to the soil respiration.

At each of the 2 slope positions, we measured soil CO₂ concentrations profiles at 4 soil depths with 3 replicates on each depth (Fig. 4). Triplicate CO₂ concentrations data were averaged, providing unique values for each depth, representative of the entire slope position. Continuous CO₂ concentrations profiles were generated by fitting a decreasing double sigmoidal model to the observations (Sect. 2.3).

As a reference, we performed surface CO₂ fluxes measurements with an infra-red gas analyzer (IRGA) linked to a survey chamber at 16 dates (profile and surface data matched in time, with a maximum time-lapse of 30 min between each other). The replicates of CO₂ concentration along soil profiles allowed catching its spatial variability at the different depths (Maier and Schack-Kirchner, 2014), extending the measurement footprint to the same area (i.e. 5 m²) than the IRGA chamber network located at the soil surface (Fig. 4). These reference surface CO₂ fluxes allowed calibrating parameters of Eqs. (1) and (4) to ensure the accuracy of profile CO₂ fluxes (Sect. 2.3).

Soil temperature was monitored using a thermistor probe (Therm107, Campbell Scientific Lt., UK). Analytical precision is 0.4 °C. Soil volumetric water content (VWC) was monitored using Time Domain Reflectometry (TDR) probes. Topp's equation (Topp et al., 1980) was used to determine VWC, from the apparent dielectric constant measured by TDR probes, as further described in Wiaux et al. (2014c).

Water, temperature and CO₂ concentration profiles measurements were recorded with an automatic data logger (CR1000, Campbell Scientific Lt., UK), connected to a multiplexer (AM16/32, Campbell Scientific, Campbell Scientific Lt., UK).

13704

In contrast to other studies (e.g. Pingingtha et al., 2010; Turcu et al., 2005), soil CO₂ diffusivity was not aggregated for the entire soil profile or for an entire soil layer, but its vertical distribution was accounted for. Eq. (4) was inserted in Eq. (1), and Eq. (1) was numerically evaluated using a depth increment of 0.1 cm. The surface CO₂ flux obtained with the gradient-based method was considered as being the top of the calculated CO₂ flux profile using Eq. (1).

2.4 Data treatments and adjustments

To optimize the quality of the soil concentration data time-series, observations corresponding to battery voltage lower than 11.5 V were removed. Soil profile CO₂ concentrations measurements were a posteriori corrected for temperature variations using the empirical formulas described by Tang et al. (2003). This allowed removing the impact of temperature on the CO₂ reading of the CO₂ probe, since the CARBOCAP® technology is temperature dependent. Probe specific parameters values for these correction formulas were provided by the probe manufacturer (Vaisala corp., Vantaa, Finland).

Triplicate VWC and CO₂ concentrations data were averaged, providing unique values for each depth, representative of the entire slope position. Soil temperature and VWC profiles were calculated using a linear interpolation between the depth specific values. Surface values were not extrapolated, and were considered as being equal to the closest observations in the profiles. CO₂ concentrations profiles were generated by fitting a decreasing double sigmoidal model to the observations as described in the previous sub-section. The performance of this model (Eq. 2) was evaluated using the regression coefficient (R^2). When R^2 values of the fitted CO₂ profiles were lower than a threshold value of 95 %, the gradient of CO₂ concentration was considered as unreliable and CO₂ fluxes were not calculated at that time.

We calibrated the diffusion model by adjusting the parameters related to the gas diffusion coefficient (i.e. b and ε_{100} such that calculated fluxes fit punctual CO₂ fluxes observations. These observations were obtained by means of a portable infra-red gas analyzer with an automated closed dynamic chamber (LI-8100A system, LI-COR, United

13707

States), following Davidson et al. (2002). The sampling design of these surface chamber CO₂ fluxes measurements on the same study site has been described in Wiaux et al. (2014 b). The regression coefficients of the relationship between both measured surface chamber and calculated CO₂ fluxes ensure the consistency (and consequently the precision) of the calculated fluxes (i.e. $R^2 = 92$ % both in 2012 and 2013). The slope of the fit (i.e. 1.05 and 1.22, respectively in 2012 and 2013) was used to correct the calculated fluxes and to ensure accuracy, as explained in Wiaux et al. (2014c).

CO₂ fluxes, as assessed by the gradient based method, were calculated on an hourly time-scale, and then integrated on a daily basis. Temperature, VWC, diffusivity and CO₂ concentration values were so averaged on a daily basis.

2.5 Vertical partitioning of CO₂ fluxes

The space-continuous CO₂ fluxes profiles obtained using Eq. (2) were partitioned into 10 slides of 10 centimeters along the soil profile. For each soil slide, we calculated the difference between top and bottom fluxes. This difference was then divided by the total CO₂ flux (e.g. the value at the soil surface). This provides the relative contribution in terms of both CO₂ production and transfer (in %) of each soil slide to the surface CO₂ flux (e.g. Goffin et al., 2014; Maier and Schack-Kirchner, 2014).

In order to allow an easy representation of the temporal dynamic of this vertical partitioning, values were averaged on semi-seasonal time-scale. Standard deviation values reflect the variability in time during each semi-season.

2.6 Interpolation and aggregation of CO₂ fluxes in time and space

Field measurements were carried out during limited time periods, and hence would not allow assessing the C budget at the whole year scale. In order to obtain continuous time-series covering the entire yearly periods, an OC dynamics model was used as a tool to interpolate and extrapolate measured data of VWC, temperature and CO₂ fluxes for the period of 3 years (2011–2013). Then, we integrated the daily simulated

13708

CO₂ fluxes for each of the three studied years. These yearly CO₂ fluxes were averaged over the three studied years and compared between slope positions. The mean yearly CO₂ flux obtained at the summit position was considered to be representative of a non-sloping landscape. To calculate mean yearly CO₂ fluxes representative of a hilly landscape, we calculated a weighted average CO₂ flux of the summit and the footslope, thereby considering the fact that the footslope colluvium represents ca. 35 % of the surface area of the studied hillslope.

2.6.1 Description of the SoilCO₂-RothC model

The SoilCO₂-RothC model has been described in detail by Herbst et al. (2008). The model combines the coupling of a one-dimensional water, heat and CO₂ flux model (SOILCO₂) with a pool concept of carbon turnover (RothC) for the prediction of soil respiration. The performance of this model was previously evaluated by Herbst et al. (2008) based on a 8 years data set of CO₂ fluxes measurements, and its predictions were judged to be acceptable (with a difference of 0.007 g C m⁻² d⁻¹ between measured and simulated mean daily respiration rates).

This model was run on a daily time step for a period of three years (2011–2013), both for the summit and the footslope positions. Other temporal resolutions (i.e. hourly and weekly time steps) were evaluated but provided poor results.

The unsaturated soil water flux is described by the Richards equation, and both the soil water capacity and unsaturated hydraulic conductivity function are calculated according to Van Genuchten (1980). Heat transport is implemented according to Simunek and Suarez (1993). Transport of soil CO₂ is simulated considering diffusion and convection in the gas phase, as well as dispersion and convection in the liquid phase. For CO₂ diffusion in the gas phase, we implemented the new Moldrup et al. (2000) model (Eq. 4) which was shown to be appropriate for calculating CO₂ fluxes (Davidson et al., 2006; Goffin et al., 2014; Wiaux et al., 2014c).

For the production of CO₂, we only considered two different OC pools on the five ones allowed by the RothC model concept. First, all OC pools in our soils were sup-

13709

posed to participate to C dynamic processes, and hence the inert organic matter (IOM pool) was kept to zero. Then, we assumed the absence of both fresh and resistant plant material (DPM and RPM pools). Hence, the RPM pool was kept to zero, while the DPM pool, characterized by a high decomposition rate constant, was used to represent the labile OC pool (NaOCl-extracted OC, as defined in Sect. 3 for the soils studied here). As we did not discriminate here between primary (i.e. vegetal origin) and secondary (i.e. microbial origin) sources of OM, the biomass concentration (BIO pool) was supposed to be included in the labile OC pool, and hence kept to zero. The stable OC pool (NaOCl-resistant OC, as defined in Sect. 3 for the soils studied here) was represented in the RothC model by the humus pool (i.e. HUM) which has a low decomposition rate constant. Reduction factors functions are used to simulate the effect of CO₂ concentration, water pressure head, and temperature on the CO₂ production according to the original version of the SOILCO₂ model, as described by Simunek and Suarez (1993).

For the boundary conditions for the soil hydrological balance, we used meteorological data, i.e. precipitation and evapo-transpiration at the top of the soil profiles, and a free drainage concept at the bottom of the soil profiles. Precipitations were directly measured in a meteorological station close to our study site (ca. 2 km). At the summit, we considered a run-off production once input water flux exceeds the infiltration capacity, while at the footslope we specified that water can accumulate at the soil surface. Daily evapo-transpiration was calculated according to the Penmann-Monteith equation, based on measured meteorological data. The boundary conditions of soil heat flow were defined using directly measured soil temperature both at the top and at the bottom of the soil profile.

2.6.2 Model parametrisation and calibration

In this study, 5 soil depth increments were considered for the two studied soil profiles, i.e. 0–18, 19–30, 31–45, 46–70, and 71–100 cm depth. These increments were chosen to consider the depths where measurements probes were installed and the soil structural properties (Wiaux et al., 2014a). The soil hydrodynamic parameters of the van

13710

Genuchten – Mualem function (Mualem, 1976; van Genuchten, 1980), as well as parameters related to the gas diffusion coefficients (i.e. b and ε_{100}) are specified for each soil material. The initial concentration of the labile and stable OC pools were specified for each soil material, as presented in Wiaux et al. (2014a).

5 For identifying the value of input parameters, we calibrated the model using the global inversion model PEST (e.g. Gallagher and Doherty, 2007). We used measured soil VWC, temperature and CO₂ concentration measurements, as well as calculated CO₂ fluxes within the profile to invert the model.

We carried out a simple sensitive analysis of the SOILCO₂-RothC model to identify 10 key parameters. Among the more sensitive parameters, which could significantly impact the outputs of the model, we firstly inverted the 9 soil Mualem – van Genuchten parameters, related to VWC, both at the summit and at the footslope. In a second step, we kept them fixed and inverted parameters related to soil CO₂ fluxes, both at the summit and the footslope: (i) the 5 initial concentrations of the labile OC pool, (ii) the 15 decomposition rate of the labile OC pool, (iii) the activation energy reflecting temperature sensitivity, as well as (iv) the HB1 coefficient (i.e. the value of the pressure head at which CO₂ production by soil micro-organisms is at the optimal level). Initial concentrations of the labile OC pool were inverted inside a realistic range of values (i.e. average ± 3 times the standard deviation) as compared to the previous measurements done by 20 Wiaux et al. (2014a). At the footslope, we additionally inverted the 5 ε_{100} parameters related to the gas diffusion.

3 Results

3.1 Spatio-temporal analysis of measured soil variables

25 Figure 5 shows the spatio-temporal variation of soil temperature, moisture and gas diffusion, and Fig. 6 shows the spatio-temporal variation of CO₂ concentrations and fluxes. All these values correspond to in-situ measurements during period of ca. 6

13711

months in 2013. Similar measurements have been carried out in 2012 and display similar spatio-temporal trends (data not shown).

The soil temperature (Fig. 5) does not significantly differ between the summit and the footslope, except during July (day of year 180 to 220) where temperatures are ca. 2 to 3° higher at the summit while they follow exactly the same temporal dynamic. The 5 surface mean daily temperatures vary all along the soil profiles from 4 to 28 °C at the summit, and from 4 to 28 °C at the footslope (for the period of measurements).

The space-time dynamics of soil volumetric water content (VWC, Fig. 5) differ completely between the summit and the footslope. At the footslope, soil VWC values remained inside a narrow interval (36 to 39 %) all along the soil profile during the considered period. At the summit, soil VWC varies from 23 to 34 % in the plow layer (0–30 cm 10 depth) and then increases by an absolute value of 15 to 5 % (respectively) in the rest of the soil profile. The soil at the summit position is the wettest during the early spring and the late autumn and driest in the summer. At the footslope soil VWC reaches the 15 saturation level in the early summer after an important rainfall event and then slowly decreases until the early autumn and reaches saturation again in the late autumn. Similarly, in the summer, the soil gas diffusivity (Fig. 6) reaches its maximum value at the summit while it reaches its lowest value at the footslope. Soil gas diffusivity is ca. 10 times lower at the footslope relative to the summit.

20 Soil CO₂ concentrations (Fig. 6) are ca. 3 times lower at the summit relative to the footslope. Along soil profiles, soil CO₂ concentrations increases with depth, following a double exponential trend as described in Wiaux et al. (2014c). This second exponential curve begins at ca. 50 depth, and is especially pronounced at the footslope, reflecting a shift of ca. 4 % CO₂ between 44 and 100 cm depth. The time course of soil CO₂ concentrations at both the summit and the footslope increases from spring to late summer 25 and then decreases to reach its lowest value in the late autumn.

The CO₂ fluxes (Fig. 6) were calculated based on both CO₂ concentrations and diffusivity following the method described in Wiaux et al. (2014c). These calculated CO₂ fluxes vary in the same range of values when comparing the footslope and the

13712

summit. However, the peaks do not occur at the same period from a slope position to another, with maximum CO₂ fluxes being emitted respectively during summer and autumn for the summit and the footslope. In addition, the duration of these maximum peaks differ between the summit and the footslope. Along the soil profiles, CO₂ fluxes decrease with depth and reach null values at ca. 30 cm depth at the summit and at ca. 15 cm depth at the footslope.

The distribution of the soil CO₂ fluxes in the profile is illustrated in Fig. 7. At the footslope, ca. 90 to ca. 95 % of the surface CO₂ fluxes is generated in the 10 first centimeters of the soil profile. The soil layer between 10 and 20 cm contribute for only 5 to 10 % depending of the period, and the deeper layers do not significantly contribute to the surface fluxes. At the summit, the relative contribution of the different soil layers is more dynamic in time, with a contribution of the 10 first centimeters of the soil profile ranging from ca. 80 % at the late spring, decreasing to ca. 60 % in the early summer, and reaching ca. 40 % from late summer to the late autumn. At the summit, the 30 first centimeters of the soil profile significantly contribute to surface fluxes. This contribution decreases with depth in the late spring and the early summer, but is homogeneously distributed with depth for the rest of the time. At the summit, soil layers deeper than 30 cm depth sometimes contribute for up to 20 % of the total flux, especially in the autumn. Between 40 to 50 cm depth, and 80 to 90 cm depth, some negative contribution (i.e. CO₂ uptake) up to -20 % is also observed.

3.2 Modeling of surface CO₂ fluxes

Results of the daily aggregated simulation with the SoilCO₂-RothC model are summarized in Table 1 and Fig. 6. The simulated soil temperatures and VWC represent adequately the observations (Table 1). The simulated CO₂ fluxes fit well the CO₂ fluxes in 2013, both for the summit and the footslope. This fit is less good at the footslope ($R^2 = 42\%$, Table 1) but it remains acceptable given the quite local shift between observations and model simulations (Fig. 8). This shift (model underestimation) may be explained by the contribution of soil alkalinity to soil CO₂ fluxes during specific dry

13713

events in summer (e.g. Laponis et al., 2008). Punctual surface CO₂ fluxes measurements (Licor chamber system) extended to daily values corroborate the goodness of fit (GOF) of the simulations in 2012 (Table 1 and Figs. 6 and 7).

Simulated surface CO₂ fluxes (Fig. 8) remains more or less in the same range of values (from 0 to 6 g C m⁻² day⁻¹ in 2011 and 2013, and up to 8 g C m⁻² day⁻¹ in 2012). However, the temporal dynamic differs between slope positions and between years of simulation, with a clear alternation of peaks of year 2011 and 2013. At the summit, CO₂ fluxes increases from the winter to reach their maximum during the summer and then decreases again (Fig. 8), similarly to the temporal dynamic of soil temperature (see Fig. 5 as an exemple). At the footslope, the lowest CO₂ fluxes occur in the middle of the summer of each year, while a very high CO₂ fluxes can be observed from the late summer until the early autumn in 2011 and 2013 as well as in spring of year 2011 (Fig. 8).

The time integrated CO₂ fluxes are presented in Table 2. For the considered a simulation period of 3 years, the footslope emits ca. 1.5 more CO₂-C than the summit ($p < 0.01$), which represents an additional flux of 287 ± 106 g CO₂-C m⁻² year⁻¹. The uncertainty on model simulations (given by ME values in Table 2) remains lower than the difference between slope positions for each year (Table 2). Once integrated at the hillslope scale, this means that such a loamy hillslope emit ca. 1.2 times more CO₂-C relative to a flat landscape ($p < 0.1$).

4 Discussion

4.1 Soil physical control on CO₂ emissions

The difference of the temporal dynamic of surface soil CO₂ fluxes between footslope and summit positions, as illustrated in Fig. 6, indicates that the limiting factors on flux emissions are not the same all along the hillslope. At the summit, on one hand, the dynamic of surface soil CO₂ fluxes clearly follows the temperature variations (Fig. 5,

13714

at non-ideal sites like sloping plots, Baldocchi, 2003). Hence, this supports the validity of the quantitative comparison of CO₂ fluxes between slope positions carried out in this study.

5 Focusing on CO₂ fluxes aggregated at the scale of the entire hillslope, such a loamy hillslope emits $683 \pm 36 \text{ g CO}_2\text{-C m}^{-2} \text{ year}^{-1}$ while a flat landscape would only emits $583 \pm 61 \text{ g CO}_2\text{-C m}^{-2} \text{ year}^{-1}$ (Table 2). For our study site, accounting only for soil C dynamics representative of flat landscapes would under-estimate annual soil-atmosphere CO₂ exchanges by ca. 20%. This supports similar conclusions drawn under a forest eco-system by Webster et al. (2008a), who highlighted a risk of under- or over-estimation of soil respiration at large scale reaching up to 30% when topography is not
10 accounted for. Our results provide a thorough quantification and a better understanding of the soil-atmosphere C exchanges specific to an agro-ecosystem on the loess belt in Belgium, which may be of high importance to adopt strategies to mitigate climate change.

15 The CO₂ emissions values reported in literature studies as soil heterotrophic respiration (considering that heterotrophic respiration fluxes constitute ca. 30% of the total ecosystem respiration and ca. 78% of total soil respiration, according to Suleau et al., 2011) are ranging from ca. 170 to ca. $456 \text{ g CO}_2\text{-C m}^{-2} \text{ year}^{-1}$ in similar conditions i.e. temperate loamy croplands (adapted from Boeckx et al., 2011; Kutsch et al., 2010; Paustian et al., 1990), from ca. 140 to ca. $144 \text{ g CO}_2\text{-C m}^{-2} \text{ year}^{-1}$ in forests ecosystems (adapted from Dai et al., 2012; Webster et al., 2008a), and reach ca. $1811 \text{ g CO}_2\text{-C m}^{-2} \text{ year}^{-1}$ in temperate grasslands on organic soils (adapted from Renou-Wilson et al., 2014). However, most of these studies were carried out on flat landscapes. To our
20 knowledge, no equivalent quantification of the hillslope aggregated CO₂ fluxes already exists for agro-ecosystems. The values of CO₂ emissions presented in this study are in the same order of magnitude but are slightly higher than literature studies on flat croplands (Boeckx et al., 2011; Kutsch et al., 2010; Paustian et al., 1990). This may be
25 explained by the hilly relief of this study site and the lateral transfer of soil particles en-

13719

riching the downslope area in soil OC (Wiaux et al., 2014a), inducing higher respiration rate relative to a flat uneroded position (Wiaux et al., 2014b).

The higher heterotrophic respiration at our study site compared to other temperate loamy croplands (Boeckx et al., 2011; Kutsch et al., 2010; Paustian et al., 1990) could
5 also be explained by some experimental biases: (i) a priming effect due to the land-use change (soil kept bare and undisturbed during 3 years); (ii) any heading due to the dark geotextile installed at the surface of the measurements stations; and (iii) the modest model performances in terms of predictivity (Table 1). Hence, the absolute estimation of the hillslope aggregated CO₂ fluxes in this study should be interpreted carefully, and the focus should be on the relative difference between emissions from flat and sloping
10 landscapes (i.e. 20%, Table 2).

In order to understand the impact of these findings in terms of C balance, it is important to compare these heterotrophic respiration fluxes to other soil C inputs and outputs. Among other things, soil heterotrophic respiration fluxes discussed here only constitute
15 ca. 30% of the total ecosystem respiration, also composed of aboveground and belowground autotrophic respiration fluxes (Suleau et al., 2011) which were not considered here. However, this exceeds the scope of this study and should be explored at the scale of hillslopes in future researches.

Notwithstanding these elements, our results support that, when modeling soil C dynamics and when quantifying soil-atmosphere CO₂ exchanges, this is of paramount
20 importance to consider slopes and elevation effects rather than a flat landscape, and to account for dynamic processes (e.g. lateral transfer of soil OC and heterogeneous distribution of soil VWC) occurring along hillslopes.

5 Conclusions

25 At the summit position of the studied hillslope, the time course of surface soil CO₂ fluxes clearly follows the time course of temperature (Figs. 5 and 6, maximum during the summer). At this position of the hillslope, observed soil CO₂ emissions are directly

13720

- Dai, Z., Trettin, C. C., Li, C., Li, H., Sun, G., and Amaty, D. M.: Effect of assessment scale on spatial and temporal variations in CH₄, CO₂, and N₂O fluxes in a forested Wetland, *Water Air Soil Poll.*, 223, 253–265, 2012.
- Davidson, E. A., Savage, K., Verchot, L. V., and Navarro, R.: Minimizing artifacts and biases in chamber-based measurements of soil respiration, *Agr. Forest Meteorol.*, 113, 21–37, 2002.
- Davidson, E. A., Savage, K. E., Trumbore, S. E., and Borken, W.: Vertical partitioning of CO₂ production within a temperate forest soil, *Glob. Change Biol.*, 12, 944–956, 2006.
- Doetterl, S., Six, J., Van Wesemael, B., and Van Oost, K.: Carbon cycling in eroding landscapes: Geomorphic controls on soil organic C pool composition and C stabilization, *Glob. Change Biol.*, 18, 2218–2232, 2012.
- Epron, D., Bosc, A., Bonal, D., and Freycon, V.: Spatial variation of soil respiration across a topographic gradient in a tropical rain forest in French Guiana, *J. Trop. Ecol.*, 22, 565–574, 2006.
- Eswaran, H., Van Den Berg, E., and Reich, P.: Organic carbon in soils of the World, *Soil Sci. Soc. Am. J.*, 57, 192–194, 1993.
- Eugster, W., Moffat, A. M., Ceschia, E., Aubinet, M., Ammann, C., Osborne, B., Davis, P. A., Smith, P., Jacobs, C., Moors, E., Le Dantec, V., Béziat, P., Saunders, M., Jans, W., Grünwald, T., Rebmann, C., Kutsch, W. L., Czerný, R., Janouš, D., Moureaux, C., Dufranne, D., Carrara, A., Magliulo, V., Di Tommasi, P., Olesen, J. E., Schelde, K., Olioso, A., Bernhofer, C., Cellier, P., Larmanou, E., Loubet, B., Wattenbach, M., Marloie, O., Sanz, M.-J., Søgaard, H., Buchmann, N.: Management effects on European cropland respiration, *Agr. Ecosys. Environ.*, 139, 346–362, 2010.
- Gallagher, M. and Doherty, J.: Parameter estimation and uncertainty analysis for a watershed model, *Environ. Modell. Softw.*, 22, 1000–1020, 2007.
- Goffin, S., Aubinet, M., Maier, M., Plain, C., Schack-Kirchner, H., and Longdoz, B.: Characterization of the soil CO₂ production and its carbon isotope composition in forest soil layers using the flux-gradient approach, *Agr. Forest Meteorol.*, 188, 45–57, 2014.
- Goulden, M. L., Munger, J. W., Fan, S.-M., Daube, B. C., and Wofsy, S. C.: Measurements of carbon sequestration by long-term eddy covariance: methods and a critical evaluation of accuracy, *Glob. Change Biol.*, 2, 169–182, 1996.
- Gregorich, E. G., Carter, M. R., Angers, D. A., Monreal, C. M., and Ellert, B. H.: Towards a minimum data set to assess soil organic matter quality in agricultural soils, *Can. J. Soil Sci.*, 74, 367–385, 1994.

13723

- Herbst, M., Hellebrand, H. J., Bauer, J., Huisman, J. A., Simunek, J., Weihermuller, L., Graf, A., Vanderborght, J., and Vereecken, H.: Multiyear heterotrophic soil respiration: Evaluation of a coupled CO₂ transport and carbon turnover model, *Ecol. Model.*, 214, 271–283, 2008.
- Houghton, R. A.: Why are estimates of the terrestrial carbon balance so different?, *Glob. Change Biol.*, 9, 500–509, 2003.
- Howard, D. M. and Howard, P. J. A.: Relationships between CO₂ evolution, moisture content and temperature for a range of soil types, *Soil Biol. Biochem.*, 25, 1537–1546, 1993.
- IPCC: Detection of the greenhouse effect in the observations, *Clim. Change: The IPCC Scientific Assessment*, edited by: Wigley, T. M. L. and Barnett, T. P., 239–256, 1990.
- IPCC: Clim. change: the supplementary report to the IPCC scientific assessment, edited by: Houghton, J. T. and Callander, B. A., Cambridge University Press, 1992.
- Kutsch, W. L., Aubinet, M., Buchmann, N., Smith, P., Osborne, B., Eugster, W., Wattenbach, M., Schrupf, M., Schulze, E. D., Tomelleri, E., Ceschia, E., Bernhofer, C., Béziat, P., Carrara, A., Di Tommasi, P., Grünwald, T., Jones, M., Magliulo, V., Marloie, O., Moureaux, C., Olioso, A., Sanz, M. J., Saunders, M., Søgaard, H., and Ziegler, W.: The net biome production of full crop rotations in Europe, *Agriculture, Ecosystems & Environment*, 139, 336–345, 2010.
- Lal, R.: Soil erosion and the global carbon budget, *Environ. Int.*, 29, 437–450, 2003.
- Maier, M., Schack-Kirchner, H., Hildebrand, E. E., and Schindler, D.: Soil CO₂ efflux vs. soil respiration: Implications for flux models, *Agr. Forest Meteorol.*, 151, 1723–1730, 2011.
- Maier, M. and Schack-Kirchner, H.: Using the gradient method to determine soil gas flux: A review, *Agr. Forest Meteorol.*, 192–193, 78–95, 2014.
- Martin, J. G. and Bolstad, P. V.: Variation of soil respiration at three spatial scales: Components within measurements, intra-site variation and patterns on the landscape, *Soil Biol. Biochem.*, 41, 530–543, 2009.
- Moldrup, P., Olesen, T., Schjøning, P., Yamaguchi, T., and Rolston, D. E.: Predicting the gas diffusion coefficient in undisturbed soil from soil water characteristics, *Soil Sci. Soc. Am. J.*, 64, 94–100, 2000.
- Mualem, Y.: A new model for predicting the hydraulic conductivity of unsaturated porous media, *Water Resour. Res.*, 12, 513–522, 1976.
- Paustian, K., Andren, O., Clarholm, M., Hansson, A. C., Johansson, G., Lagerlof, J., Lindberg, T., Petersson, R., Sohlenius, B.: Carbon and Nitrogen Budgets of Four Agro-Ecosystems With Annual and Perennial Crops, With and Without N Fertilization, *J. Appl. Ecol.*, 27, 60–84, 1990.

13724

- Peters, W., Krol, M. C., Van Der Werf, G. R., Houweling, S., Jones, C. D., Hughes, J., Schaefer, K., Masarie, K. A., Jacobson, A. R., Miller, J. B., Cho, C. H., Ramonet, M., Schmidt, M., Ciattaglia, L., Apadula, F., Heltai, D., Meinhardt, F., Di Sarra, A. G., Piacentino, S., Sferlazzo, D., Aalto, T., Hatakka, J., Ström, J., Haszpra, L., Meijer, H. A. J., Van Der Laan, S., Neubert, R. E. M., Jordan, A., Rodó, X., Morguí, J. A., Vermeulen, A. T., Popa, E., Rozanski, K., Zimnoch, M., Manning, A. C., Leuenberger, M., Uglietti, C., Dolman, A. J., Ciais, P., Heimann, M., Tans, P. P.: Seven years of recent European net terrestrial carbon dioxide exchange constrained by atmospheric observations, *Glob. Change Biol.*, 16, 1317–1337, 2010.
- Pingintha, N., Leclerc, M. Y., Beasley, J. P., Zhang, G., and Senthong, C.: Assessment of the soil CO₂ gradient method for soil CO₂ efflux measurements: Comparison of six models in the calculation of the relative gas diffusion coefficient, *Tellus B*, 62, 47–58, 2010.
- Quinton, J. N., Govers, G., Van Oost, K., and Bardgett, R. D.: The impact of agricultural soil erosion on biogeochemical cycling, *Nat. Geosci.*, 3, 311–314, 2010.
- Reicosky, D. C., Lindstrom, M. J., Schumacher, T. E., Lobb, D. E., and Malo, D. D.: Tillage-induced CO₂ loss across an eroded landscape, *Soil and Tillage Research*, 81, 183–194, 2005.
- Rommens, T., Verstraeten, G., Poesen, J., Govers, G., Van Rompaey, A., Peeters, I., and Lang, A.: Soil erosion and sediment deposition in the Belgian loess belt during the Holocene: Establishing a sediment budget for a small agricultural catchment, *Holocene*, 15, 1032–1043, 2005.
- Rumpel, C. and Kögel-Knabner, I.: Deep soil organic matter – a key but poorly understood component of terrestrial C cycle, *Plant Soil*, 338, 143–158, 2011.
- Šimůnek, J. and Suarez, D. L.: Modeling of carbon dioxide transport and production in soil: 1. Model development, *Water Resour. Res.*, 29, 487–497, 1993.
- Smith, S. V., Sleezer, R. O., Renwick, W. H., and Buddemeier, R. W.: Fates of Eroded Soil Organic Carbon: Mississippi Basin Case Study, *Ecol. Appl.*, 15, 1929–1940, 2005.
- Stallard, R. F.: Terrestrial sedimentation and the carbon cycle: Coupling weathering and erosion to carbon burial, *Global Biogeochem. Cy.*, 12, 231–257, 1998.
- Suleau, M., Moureaux, C., Dufranne, D., Buysse, P., Bodson, B., Destain, J.-P., Heinesch, B., Debacq, A., Aubinet, M.: Respiration of three Belgian crops: Partitioning of total ecosystem respiration in its heterotrophic, above- and below-ground autotrophic components, *Agr. Forest Meteorol.*, 151, 633–643, 2011.

13725

- Tang, J. W., Baldocchi, D. D., Qi, Y., and Xu, L. K.: Assessing soil CO₂ efflux using continuous measurements of CO₂ profiles in soils with small solid-state sensors, *Agr. Forest Meteorol.*, 118, 207–220, 2003.
- Takahashi, A., Hiyama, T., Takahashi, H. A., and Fukushima, Y.: Analytical estimation of the vertical distribution of CO₂ production within soil: application to a Japanese temperate forest, *Agr. Forest Meteorol.*, 126, 223–235, 2004.
- Topp, G. C., Davis, J. L., and Annan, A. P.: Electromagnetic determination of soil water content: Measurements in coaxial transmission lines, *Water Resour. Res.*, 16, 574–582, 1980.
- Trumbore, S. E. and Czimczik, C. I.: Geology – An uncertain future for soil carbon, *Science*, 321, 1455–1456, 2008.
- Turcu, V. E., Jones, S. B., and Or, D.: Continuous soil carbon dioxide and oxygen measurements and estimation of gradient-based gaseous flux, *Vadose Zone J.*, 4, 1161–1169, 2005.
- Van Genuchten, M. T.: A Closed-form Equation for Predicting the Hydraulic Conductivity of Unsaturated Soils, *Soil Sci. Soc. Am. J.*, 44, 892–898, 1980.
- Van Oost, K., Verstraeten, G., Doetterl, S., Notebaert, B., Wiaux, F., Broothaerts, N., and Six, J.: Legacy of human-induced C erosion and burial on soil-atmosphere C exchange, *P. Natl. Acad. Sci. USA*, 109, 19492–19497, 2012.
- Wang, Z., Van Oost, K., Lang, A., Quine, T., Clymans, W., Merckx, R., Notebaert, B., and Govers, G.: The fate of buried organic carbon in colluvial soils: a long-term perspective, *Biogeosciences*, 11, 873–883, doi:10.5194/bg-11-873-2014, 2014.
- Webster, K. L., Creed, I. F., Beall, F. D., and Bourbonniere, R. A.: Sensitivity of catchment – aggregated estimates of soil carbon dioxide efflux to topography under different climatic conditions, *J. Geophys. Res.-Biogeosci.*, 113, G03040, doi:10.1029/2008JG000707, 2008a.
- Webster, K. L., Creed, I. F., Bourbonniere, R. A., and Beall, F. D.: Controls on the heterogeneity of soil respiration in a tolerant hardwood forest, *J. Geophys. Res.-Biogeosci.*, 113, G03018, doi:10.1029/2008JG000706, 2008b.
- Wiaux, F., Cornelis, J. T., Cao, W., Vanclooster, M., and Van Oost, K.: Combined effect of geomorphic and pedogenic processes on the distribution of soil organic carbon quality along an eroding hillslope on loess soil, *Geoderma*, 216, 36–47, 2014a.
- Wiaux, F., Vanclooster, M., Cornelis, J. T., and Van Oost, K.: Factors controlling soil organic carbon persistence along an eroding hillslope on the loess belt, *Soil Biol. Biochem.*, 77, 187–196, 2014b.

13726

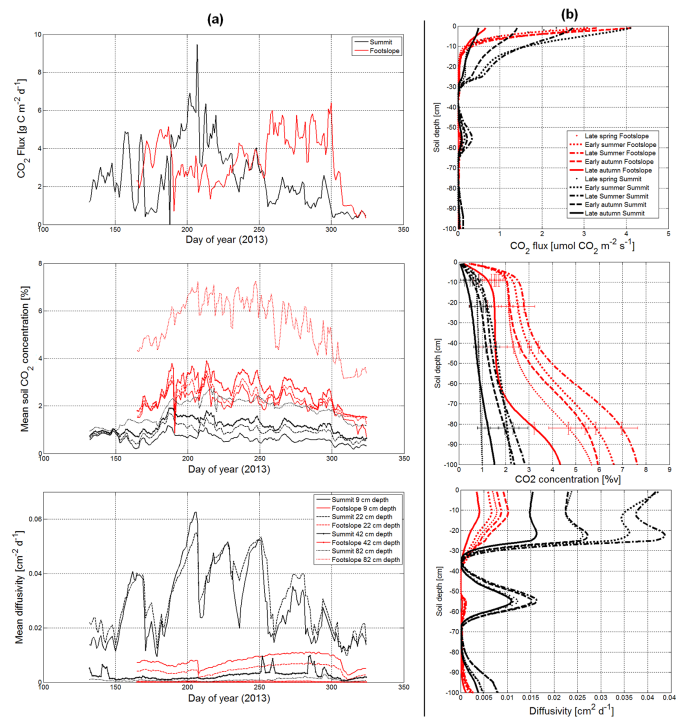


Figure 6. Space-time dynamic of soil CO₂ diffusivity, concentrations and fluxes at the summit (red) and the footslope (black) position in 2013: **(a)** time series at different depths; **(b)** profile at different dates.

13735

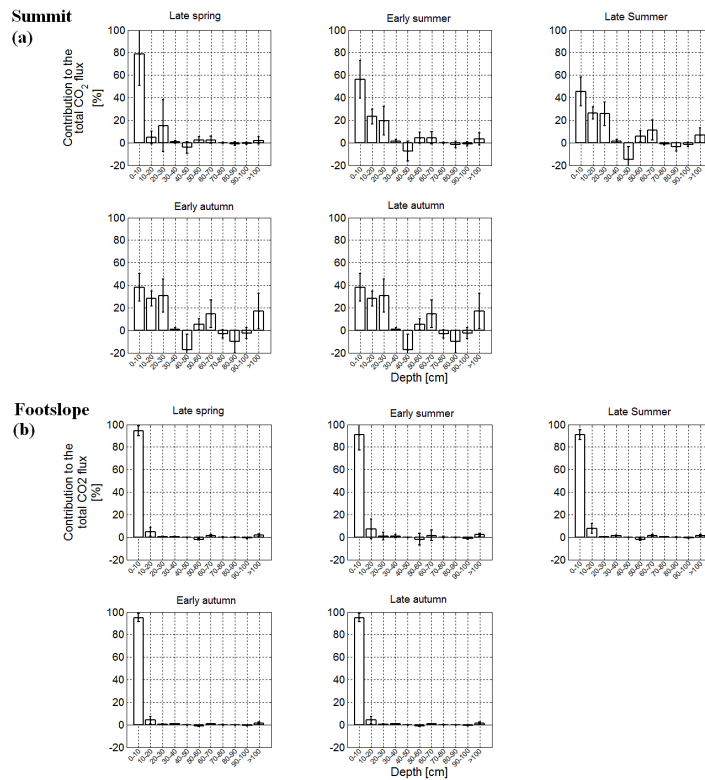


Figure 7. Depth distribution of the relative contribution to soilsurface CO₂ fluxes in year 2013 averaged by semi-seasons (error bars represent the standard deviation of the time aggregation for each soil layer): **(a)** at the summit, and **(b)** at the footslope position.

13736

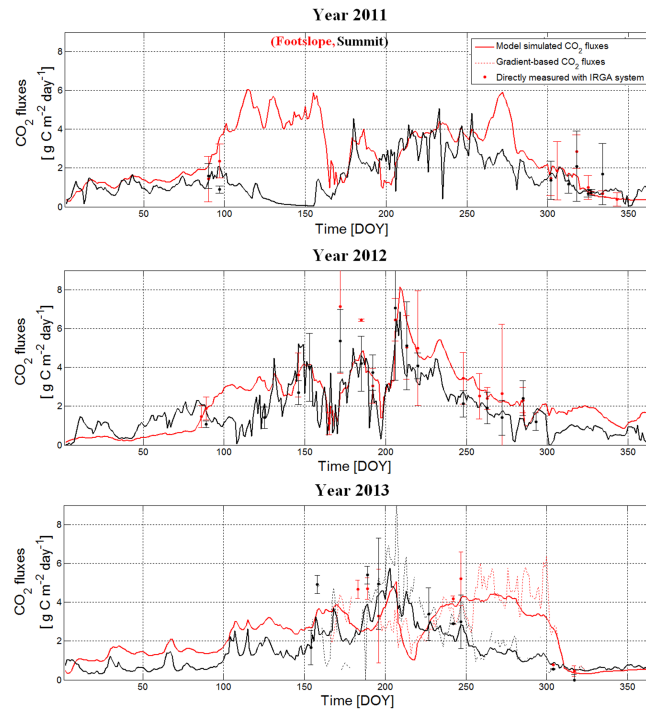


Figure 8. CO₂ fluxes from 2011 to 2013 at two slope positions (footslope in red, summit in black): **(i)** simulation based on the SOILCO₂-RothC model (plain lines), **(ii)** calculated fluxes with the gradient-based method (dashed lines), and **(iii)** spatial average of in situ measured fluxes with the IRGA Licor chamber (points with errorbars).